Proceedings of the 3rd Croatian Conference on Earthquake Engineering - 3CroCEE
19–22 March 2025, Split, Croatia

DOI: https://doi.org/10.5592/CO/3CroCEE.2025.95

MODELLING THE SEISMIC RESPONSE OF A CONFINED MASONRY BUILDING USING EQUIVALENT STRUT MODELS

Nemanja Krtinić [(1)], Matija Gams [(2)], Marko Marinković [(3)]

[(1)] *PhD student, Faculty of Civil and Geodetic Engineering, University of Ljubljana, nkrtinic@fgg.uni-lj.si*
[(2)] *Assistant professor, Faculty of Civil and Geodetic Engineering, University of Ljubljana, mgams@fgg.uni-lj.si*
[(3)] *Assistant professor, Faculty of Civil Engineering, University of Belgrade, mmarinkovic@grf.bg.ac.rs*

Abstract

Confined masonry (CM) technology is extensively employed in many parts of the world for the construction of residential buildings due to its improved seismic performance compared to the unreinforced masonry (URM). This study focuses on the numerical simulation of seismic response of CM walls and a three-storey model of a CM building using Equivalent Strut Models (ESM) in OpenSees framework. Different strut and constitutive models available in the literature were used. The primary objective is to identify the most suitable model for simulating the global response of CM walls and structures. Firstly, different numerical models of the CM wall were compared against two full-scale shear compression tests, which enabled us to identify the most suitable and accurate model. The most suitable model was then used to develop a numerical model of the three-storey CM building, and the results of the simulations were compared with the experiment.

Keywords: confined masonry, equivalent strut model, numerical modelling, pushover analysis, OpenSees.

1. Introduction

The European masonry industry is developing new products and construction technologies that offer improved thermal properties, thereby reducing energy consumption for heating and cooling, while also enhancing the comfort of occupants. One such technology involves the use of polyurethane (PU) adhesive instead of thin-bed mortar, which reduces joint thickness to almost zero, preventing heat transfer through the joints. Additionally, this technology enables faster construction and building at lower temperatures. Typically, the PU glue is applied only in bed-joints, while head joints remain unfilled. Masonry blocks are also evolving, with new types featuring larger cavities filled with insulation material, which further reduces thermal conductivity of walls. This construction technology is often employed in the seismic-prone regions, such as Southeastern Europe, where masonry structures are built using confined masonry (CM) technology with reinforced concrete (RC) vertical and horizontal tie-elements, also known as tie-columns and tie-beams, respectively.

The seismic response of CM built with the new type of masonry, incorporating new masonry products and construction with PU glue, was recently experimentally tested through shear-compression tests on two full-scale CM wall test specimens under constant compressive loading [1], as well as by investigating a three-storey full-scale CM building [2]. Numerical modelling of this type of masonry is relatively poorly researched. However, modelling is a promising alternative to expensive and challenging full-scale experiments, offering a valuable complement to and extension of experimental research. Numerical approaches for seismic analysis of CM structures vary, ranging from detailed micro models to simplified micro models and macro models, with the choice depending on the objectives of the analysis and the required level of detail. The Equivalent Strut Model (ESM) is a widely used macro-modelling approach that balances accuracy and computational efficiency, making it suitable for routine design.

The main objective of this study is to numerically model the seismic response of CM walls using equivalent diagonal strut models. To identify the most suitable mathematical model, three different

DOI: https://doi.org/10.5592/CO/3CroCEE.2025.95

constitutive laws were applied to the single ESM models. These numerical 2D models were developed using the open-source software OpenSees [3].

First, numerical simulations of CM walls were conducted, and by comparing the results with experimental results, the most suitable model was identified. The selected model was then used to numerically simulate the seismic response of the three-storey CM building. The aim of the study is to evaluate whether equivalent strut models, which are simple enough for practical use, can accurately and reliably represent the global response of walls and buildings constructed with the previously described new type of CM.

2. Brief overview of the previous experimental campaigns

2.1. Walls

Two confined masonry (CM) walls, labelled W7 and W8, were tested in a laboratory, as detailed in [1]. Both walls were built with identical dimensions: 175 cm in length, 195 cm in height, and 38 cm in thickness (Fig. 1a). The tie-columns measured 25 x 25 cm (Fig. 1b), and were reinforced with 4 Ø 14 mm bars, providing a longitudinal reinforcement ratio of 1 %. The transverse reinforcement consisted of Ø 8 mm stirrups spaced approximately 20 cm apart. The dimensions of the vertical tie-columns exceeded the requirements outlined in Eurocode 8/1 [4], while the reinforcement complied with the Eurocode 8/1 requirements, which mandate at least 1 % longitudinal reinforcement and transverse reinforcement of at least Ø5/15 cm.

A notable feature of these CM walls is that the tie-columns do not cover the full thickness of the wall. Specifically, they are positioned flush with one surface of the masonry, while on the opposite side, they are depressed by 13 cm, as shown in Fig. 1a.

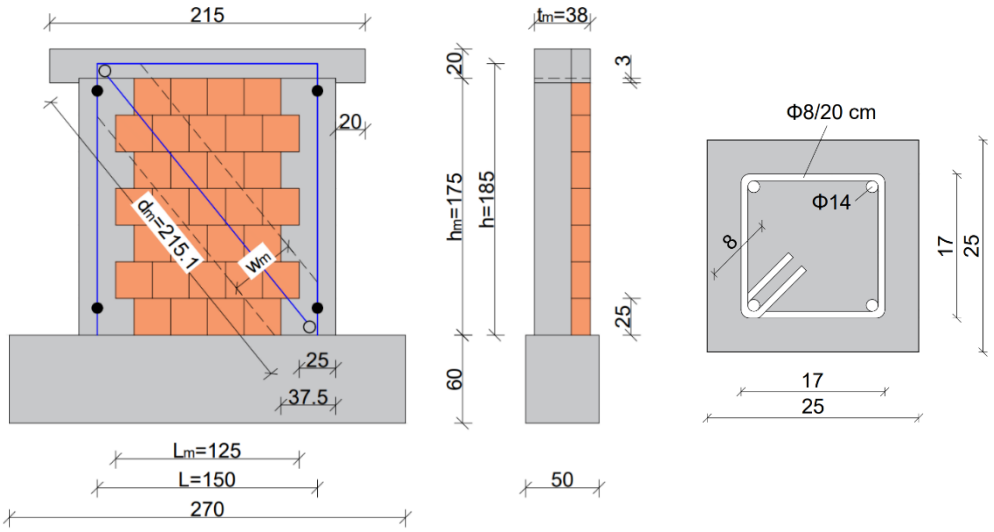

Figure 1: a) CM wall test specimen (dimensions in cm); b) Tie-column reinforcement [1].

2.2. Three-storey masonry building

The three-storey CM building model, tested at nearly full scale in a laboratory, is detailed in a separate study by Gams et al. [2]. The floor plan dimensions of the building were 5.6 x 3.9 m (Fig. 2a), and due to the spatial limitations of the laboratory, the storey height was reduced to 2.15 m, with a clear storey height of 2.0 m. The thickness of the RC floor slabs was 15 cm. The model was doubly symmetric, with two shear walls loaded in their plane and two cross walls providing stability. Cross walls are fully confined with tie-columns at both ends of piers. The shear walls consisted of three piers and two openings, each measuring 0.9 x 1.75 m (Fig. 2b). The central pier, which was longer than the side piers,

DOI: https://doi.org/10.5592/CO/3CroCEE.2025.95

had a length of 1.75 m. Note that the central pier and tie-columns were identical to those used in walls W7 and W8 (placed on both sides). The shorter piers had tie-columns only on one end due to their length of about 1m. Above the openings, lintels with dimensions of 25 x 25 cm were placed, with longitudinal reinforcement consisting of four Ø14 bars and stirrup reinforcement of Ø8/20 cm.

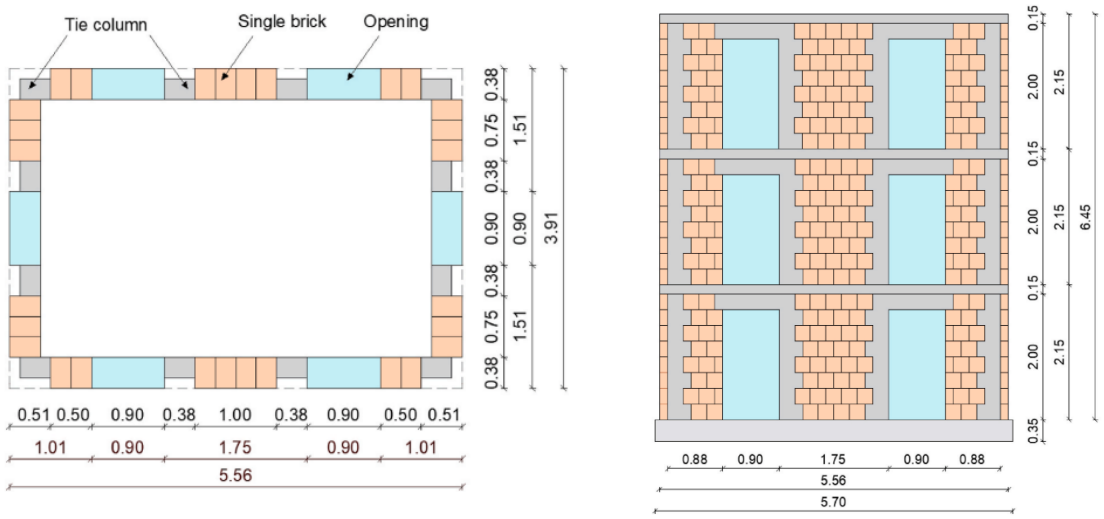

a) b)

Figure 2: Plan of the three-storey building: a) floor plan, b) side view [2]. All dimensions are in meters.

2.3. Brief overview of the test results

The walls W7 and W8 were tested under in-plane shear compression conditions, with a constant vertical stress of 0.63 MPa. Fixed-fixed boundary conditions were applied (no rotation at the top, with constant vertical force), while horizontal displacements were cyclically applied at the bond beam level. Each displacement amplitude was repeated three times in both directions to simulate seismic loading in a standard manner [5]. The displacement amplitude was progressively increased until near-collapse. The amplitude was gradually increased until nearing collapse. A Digital Image Correlation (DIC) system was used to measure displacement and strain fields across the surface of the wall. Further details regarding the experimental setup, instrumentation, loading protocol, and comprehensive test results are provided in [1].

Fig. 3a shows the hysteretic response envelopes for both walls, obtained as the average response in both the push and pull directions. The envelopes also highlight different limit states (LSs): the green circle represents the damage LS, the blue circle indicates the maximum resistance LS, and the red circle marks the near-collapse LS.

The seismic response of the tested CM walls was as expected, with dominant shear behaviour. However, the observed damage was unexpected. An interesting phenomenon occurred at the interface between the masonry and tie-columns, where initial cracking initiated by tie-columns and damage spread towards the centre of the wall. This damage was primarily caused by the geometry of the blocks, which featured larger individual holes (6 % of the total volume), and a total hole volume of 59 %. These values exceed the Eurocode 6 [5] limits for load-bearing walls (2 % and 55 %, respectively). The protruding part of masonry, which was not fully confined by tie-columns, was significantly damaged already at the maximum resistance LS (at about 0.5 % drift) and completely sheared off at a drift of 1.3 % (Fig. 3b).

DOI: https://doi.org/10.5592/CO/3CroCEE.2025.95

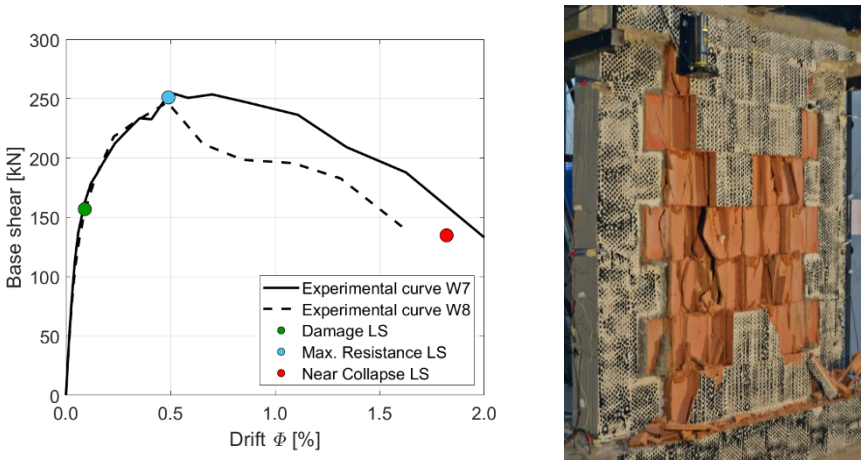

a) b)

Figure 3: a) Experimentally obtained envelope curves of the two tested CM walls W7 and W8, with marked limit states; b) Cracking in the plane of the wall due to tie-columns at 1.3 % drift.

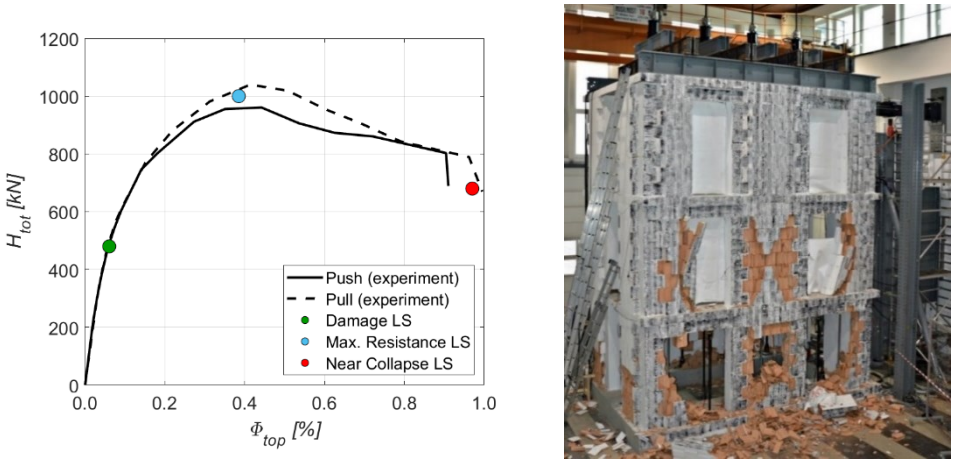

a) b)

Figure 4: a) Experimentally obtained envelope curve (base shear against top drift) of a three-storey masonry building with highlighted limit states; b) Masonry building close to the Near Collapse LS.

The three-storey building model was tested in the same manner as CM walls. First, a vertical load was applied to the model, inducing a compressive stress state of approximately 0.63 MPa in the walls, corresponding to about 20 % of the characteristic compressive strength of the masonry (f_k). This vertical stress was caused by a total force of 2395 kN. Part of this force was contributed by the self-weight of the walls and floor slabs, while the remaining portion was applied using four hydraulic actuators positioned at the top of the building. After the vertical load was applied, the building was subjected to a cyclic lateral load with an inverted triangular distribution, applied three times for each load level. The test was displacement-controlled at the first storey, and the measured force in the first storey was scaled accordingly for the upper two stories. The hysteretic response envelope, shown separately for pushing and pulling direction, is presented in Fig. 4a, with limit states indicated by the same symbols used for the walls. The damage LS was reached at a drift of 0.07–0.08 %, while the significant damage LS was observed at a drift of 0.55 %. The near-collapse LS, indicating the building was close to the failure, was reached at a drift of 1 % for the entire structure, and at 1.75 % drift for the bottom storey (see Fig. 4b).

DOI: https://doi.org/10.5592/CO/3CroCEE.2025.95

3. Numerical macro-modelling

In this Section, the classical model with an equivalent diagonal strut [7] is used to simulate the global seismic response of walls and buildings built using CM technology. Although the ESM model was originally developed for reinforced concrete (RC) frame structures with infills, it can be adapted for CM structures (see e.g., [5], [8]). Since the model is relatively simple, it is also suitable for practical applications. The main drawback is that the model is unable to capture local phenomena, which are often not of interest in design.

The model of the RC members and the strut for CM walls used in this work is essentially the same as that for RC frame structures with infills, except that plastic hinges are assumed not to develop in the bond beam. This is because the masonry and the top beam are strongly connected (the concrete is poured directly onto the masonry), and because no such damage was observed during the tests. In this paper, three commonly used simple ESMs with one single strut are applied, namely the models of Panagiotakos and Fardis model [9], the Decanini et al. model [10], and the Liberatore et al. model [11]. Since a detailed description of each model exceeds the scope of this paper, only brief descriptions and the calculated characteristic points of the strut models are provided, in the form of graphs of strut force–strut displacement.

The ESM model of the considered CM walls is shown in Fig. 1a, where L is the length of the wall measured between the central axes of the tie-columns, L_m is the length of the masonry panel, h is the specimen height, h_m is the height of the masonry panel, w_m is the width of the equivalent strut, d_m is the length of the equivalent strut, t_m is the masonry wall thickness, and θ is the inclination angle of the strut.

3.1. Equivalent strut models

3.1.1. Model by Panagiotakos and Fardis [9]

The classical ESM describes the behaviour of strut with four linear segments, as shown in Fig. 5. The initial state is followed by the cracked state up to the point of maximum resistance. After that, there is a segment of strength degradation, eventually leading to residual strength. The graph shows only the response of the wall panel without the contribution of the RC ties. The characteristic points of the strut, calculated for walls W7 and W8, are summarized in Table 1.

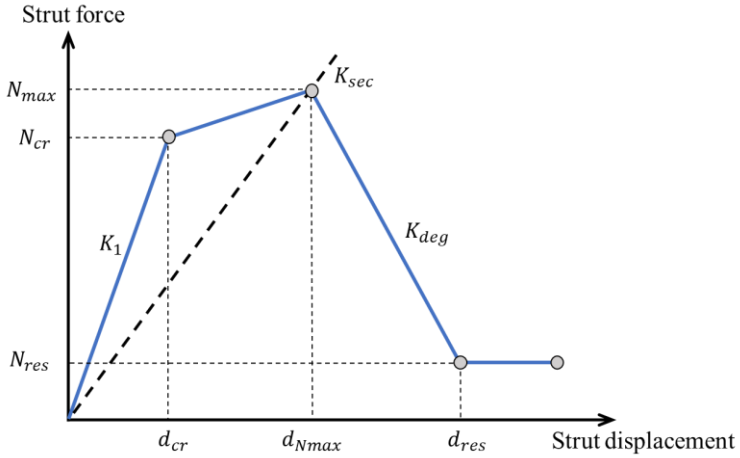

Figure 5: Constitutive model of the strut [9].

Proceedings of the 3rd Croatian Conference on Earthquake Engineering - 3CroCEE
19–22 March 2025, Split, Croatia

DOI: https://doi.org/10.5592/CO/3CroCEE.2025.95

Table 1: Characteristic points of the ESM model according to the model of Panagiotakos and Fardis [9]

Limit state	**Strut displacement *d* [mm]**	**Wall drift *Φ* [%]**	**Strut force *N* [kN]**
Crack	0.34	0.03	237.0
Max. resistance	3.41	0.32	308.1
Residual	11.25	1.05	30.8
Ultimate	34.87	3.24	30.8

3.1.2. Model by Decanini et al. [10]

The constitutive law of the equivalent strut proposed by Decanini et al. [10] is also composed of four linear segments (see Section 3.1.1, Fig. 5). The key difference lies in how the characteristic points are calculated. The most notable difference is in the calculation of the maximum resistance $N_{\max}$, which, in the case of the Decanini et al. [10] model, requires evaluating four different failure mechanisms and selecting the most critical one.

The critical stresses for all four mechanisms are shown in Table 2.

Table 2: Estimation of the failure stress in the masonry panel [10]

Equation	**Stress [MPa]**	**Failure mode**
$\sigma_{m,a} = \dfrac{1.16 f_{md} \tan\theta}{K_1 + K_2 \lambda_h} t_w d$	8.31	Diagonal compression failure
$\sigma_{m,b} = \dfrac{1.12 f_{md} \sin\theta \cos\theta}{K_1 (\lambda_h)^{-0.12} + K_2 (\lambda_h)^{-0.88}}$	3.13	Corner crushing
$\sigma_{m,c} = \dfrac{(1.2\sin\theta + 0.45\cos\theta) f_{v0} + 0.3\sigma_V}{w_m / d_m}$	1.57	Sliding of bed joints
$\sigma_{m,d} = \dfrac{0.6 f_{md} + 0.3\sigma_V}{w_m / d_m}$	1.63	Diagonal tensile failure

* σ_V is the vertical compressive stress in the masonry panel (equal to 0.63 MPa). The tensile strength of the masonry was evaluated from tests conducted for this purpose and $f_{md} = f_{mt}$ is equal to 0.29 MPa [1].

$$N_{\max} = t_m \cdot b_m \cdot \min\left(\sigma_{m,a}, \sigma_{m,b}, \sigma_{m,c}, \sigma_{m,d}\right) \tag{1}$$

The values in the middle column of Table 2 indicate that the critical failure mechanism is sliding along the bed joints. However, the actual tests revealed that the CM walls failed due to diagonal tensile cracking. Since the difference in prediction for both failure modes is only 0.06 MPa, the discrepancy is not crucial for the model of Decanini et al. [10]. The maximum resistance of the strut based on Eq. (1) is 286 kN. The remaining characteristic values of the strut model are shown in Table 3.

Table 3: Characteristic points of the ESM model according to the model of Decanini et al. [10]

Limit state	**Strut displacement *d* [mm]**	**Wall drift *Φ* [%]**	**Strut force *N* [kN]**
Crack	0.23	0.02	228.8
Max. resistance	1.54	0.14	286.0
Residual	26.56	2.47	100.1
Ultimate	29.06	2.70	100.1

Proceedings of the 3rd Croatian Conference on Earthquake Engineering - 3CroCEE
19–22 March 2025, Split, Croatia

DOI: https://doi.org/10.5592/CO/3CroCEE.2025.95

3.1.3. Model by Liberatore et al. [11]

The ESM model proposed by Liberatore et al. [11] is based on the statistical analysis of 162 experimental results and consists of four linear segments with four characteristic points, as shown in Fig. 6. Unlike earlier ESM models, it provides explicit values for the displacements corresponding to these points, rather than deriving them through equations describing mechanical behaviour. This allows the model to scale these points according to the material properties of the masonry.

The strut properties are calculated by determining the reference strength $N_{max,ref}$ following the procedure outlined in Section 3.1.2. For the analysed walls, this value is 286.0 kN. The remaining characteristic points of the constitutive law are calculated using regression coefficients provided in [11]. As an example, it is shown only the calculation of the maximum resistance, which requires only a modification for vertical holes and it is modified with the parameter 0.98 [11]:

$$N_{max} = 0.98 \cdot N_{max,ref} \tag{2}$$

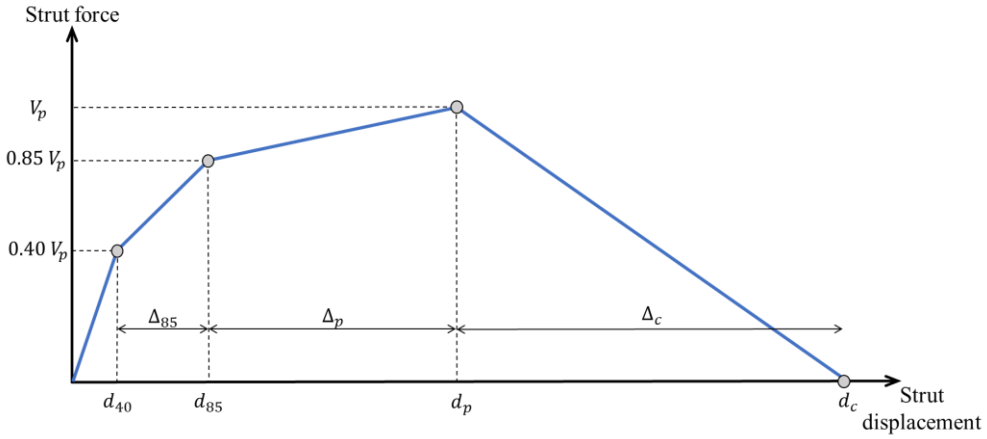

Figure 6: Constitutive model of the strut [11].

The characteristic points of the strut model by Liberatore et al. [11] for CM walls are given in Table 4.

Table 4: Characteristic points of the ESM model according to the model of Liberatore et al. [11]

Limit state	**Strut displacement *d* [mm]**	**Wall drift *Φ* [%]**	**Strut force *N* [kN]**
Crack	0.25	0.02	112.1
Max. resistance	2.31	0.21	238.2
Residual	5.45	0.51	280.3
Ultimate	35.97	3.34	0

3.1.4. Comparison of the ESM models

The constitutive material models of the ESMs are shown in Fig. 7. While good agreement is shown in terms of maximum resistance, significant differences are observed in other aspects. The largest differences appear in the degradation part of the curves (the slope after reaching the maximum load capacity), where the model by Panagiotakos and Fardis stands out significantly. The models by Liberatore et al. and Decanini et al. show the most significant differences within the range between the initial cracking and the maximum load capacity state.

DOI: https://doi.org/10.5592/CO/3CroCEE.2025.95

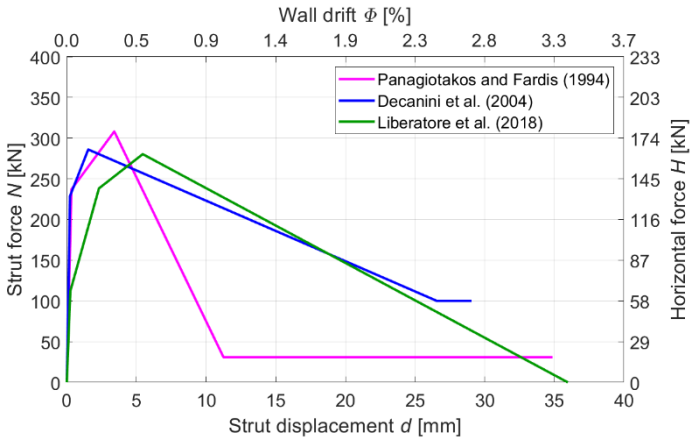

Figure 7: Comparison of the strut force–strut displacement (horizontal force–wall drift) curves for ESMs proposed by various authors.

3.1.5. Numerical model and validation

The numerical model of the CM wall was built in the OpenSees software package [3]. In the ESM model, the RC ties (tie-columns and bond beam) are represented as RC frame elements, while the masonry wall is modelled using pin-joined diagonal strut element (Fig. 8a). The strut element in the model shown in Fig. 8a has a nonlinear relationship between wall resistance (axial force) and (axial) displacement. The vertical load on the vertical RC tie-elements was determined based on the stiffness ratio between the masonry panel and the vertical ties (in the model, vertical force acts only on the ties) and was set to 150 kN per tie-column. After applying the vertical force, the wall was loaded with a monotonically prescribed horizontal displacement in the upper left corner (Fig. 8a) up to the same drift as in the experiment. The P-Delta effects were included in the static nonlinear analysis.

The tie-columns were fixed at the base, and modelled using the "*Beam With Hinges*" (BWH) *element*, which assumes that plastic hinges can only form at the ends of the elements. The length of the plastic zone (plastic hinge length) was calculated according to the recommendations in Eurocode 8-3 [12]:

$$L_{pl} = \frac{L_v}{30} + 0.2h + 0.11\frac{d_{bL} f_y}{\sqrt{f_c}} = 23.6 \text{ cm} \tag{3}$$

where L_v is the shear span (assuming a contra-flexure point at the mid-height of tie-column), h is the depth of the cross-section, f_c is the concrete compressive strength, and f_y and d_{bL} are the yield strength and the diameter of longitudinal bars, respectively.

Since no damage was observed in the bond beam and because the displacement of the bond beam was prevented by the masonry at the bottom and by the steel support at the top, the bond beam was modelled as an elastic element (*Elastic Beam Column Element* in [3]).

DOI: https://doi.org/10.5592/CO/3CroCEE.2025.95

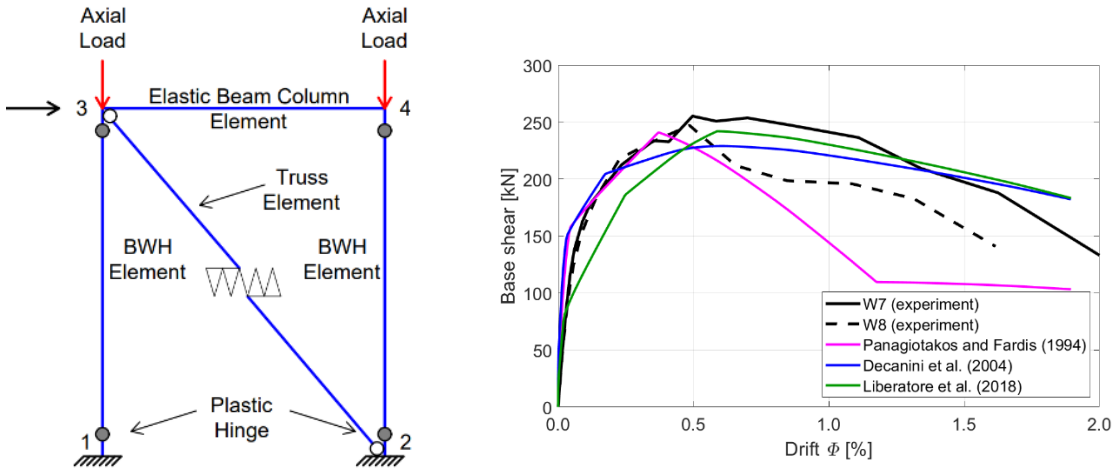

a) b)

Figure 8: a) Schematic representation of the 2D ESM for considered CM wall; b) Comparison of numerical simulations with experimental results.

The cross-section of the tie-columns was modelled using a fibre section with special fibres for the longitudinal bars. Given that the stirrups were Ø8 spaced at approximately 20 cm, the effect of confinement was negligible, and the entire section was treated as unconfined. For concrete, the material model Concrete01 [3] without tensile strength was used, as presented in Fig. 9a. The steel bars were modelled using the Steel02 model with a hardening ratio of 0.55 % (Fig. 9b). The nonlinear behaviour of the equivalent single strut in the form of strut force-strut displacement was modelled using the *Pinching4* model, which allows the definition of the multi-linear curve with four points.

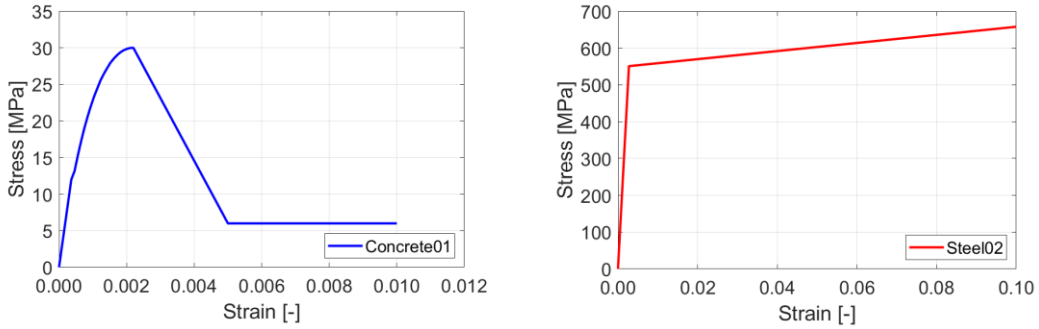

a) b)

Figure 9: Uniaxial material response: a) concrete and b) steel.

The comparison between numerical simulations and the experimental envelope curves is shown in Fig. 8b. The numerical (magenta) curve represents the model of Panagiotakos and Fardis model [9], which slightly overestimates the initial stiffness compared to the experiment (solid and dashed black lines) but accurately predicts the maximum load capacity of the CM wall. However, it underestimates the drift at peak load capacity by 25 % and predicts faster degradation than observed experimentally.

The blue curve, based on Decanini et al. model [10], slightly overestimates the stiffness and underestimates the maximum load capacity by 10 %, as seen in Fig. 8b. It should be noted that the numerical curve aligns well with the experimental response in terms of stiffness degradation.

The prediction of the Liberatore et al. model [11] is shown in Fig. 8b with the green curve. While the model accurately predicts the maximum load and load degradation, the model poorly captures the

DOI: https://doi.org/10.5592/CO/3CroCEE.2025.95

behaviour from the initial crack to the peak load stage. The model predicts the maximum load capacity at 0.58 % drift, while in the experiment it was achieved at 0.5 %.

Overall, the Decanini et al. model [10] provides the closest match and was selected as the most suitable for numerically modelling the seismic response of a three-storey masonry building.

3.3. Numerical model of a three-storey masonry building and results

Since the building's response was primarily translational, the numerical model of a three-storey masonry building was simplified by modelling only one shear wall and half of the cross walls (see Fig. 2a). The tie-columns from the cross walls incorporated into the RC ties at the extreme left and right edges of the considered shear wall. As only half of the building was modelled, the calculated load capacity was doubled to account for the entire structure.

The 2D numerical model of the building, shown in Fig. 10, was developed similarly to the CM wall model (see Fig. 8a). The masonry wall was represented using equivalent struts with a nonlinear response. It was observed during the experiment that the failure of the edge piers (confined on only one side) occurred at a drift of 0.5 %, and this was also incorporated into the numerical model. The vertical RC tie-elements were modelled as line elements with plastic hinges. Since minor cracks were observed during the test in the horizontal RC ties above the openings, the tie-beams were modelled using elements with plastic hinges in these regions. The parts of the horizontal RC ties above the piers were modelled using “rigid” elements (see Fig. 10).

The vertical load was applied to the numerical model first, followed by the application of the horizontal load, in accordance with the experimental setup. The load was distributed in a triangular pattern along the building height, and, as in the experiment, the displacement was applied at the first-floor level.

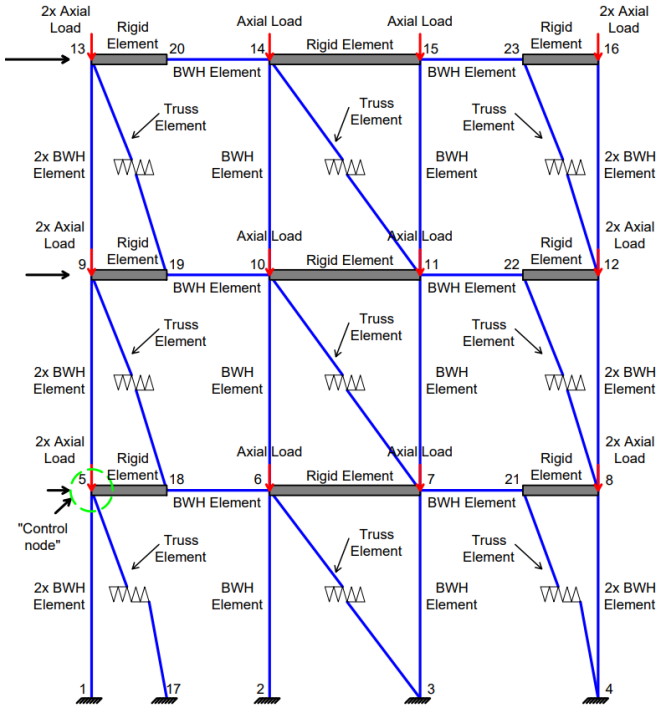

Figure 10: Numerical model of the three-storey CM building.

Fig. 11 presents a comparison between the numerical simulation and the experimentally obtained envelope curves for both directions in terms of a pushover curve. The simulation slightly overestimates the initial stiffness and reaches the maximum load at a drift of 0.37 %, whereas the drift reached during the experiment was 0.44 % (pushing) and 0.41 % (pulling). The peak capacity predicted by the model

DOI: https://doi.org/10.5592/CO/3CroCEE.2025.95

was nearly aligned with the experimental load capacity, with a minor underestimation of 3 % in the pushing direction and 10 % in the pulling direction.

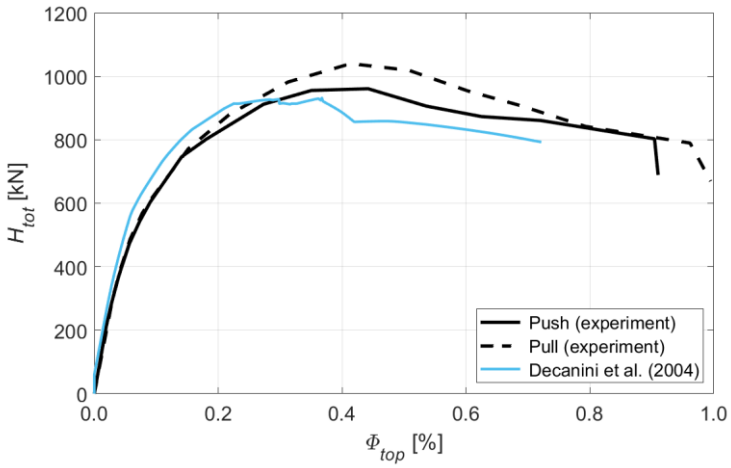

Figure 11: Comparison of the numerical simulation and the experimental response of the three-storey building.

The comparison of the building responses for each individual floor is shown in Fig. 12. The response of the ground floor in Fig. 12a shows a very good match between the simulation and the experiment, indicating that damage concentration and eventual failure occur in the ground floor. However, the response in the upper floors (Fig. 12b and Fig. 12c) shows a significant deviation from the experimental results. The issue with the model is that the upper floors are relieved when damage occurs in the ground floor.

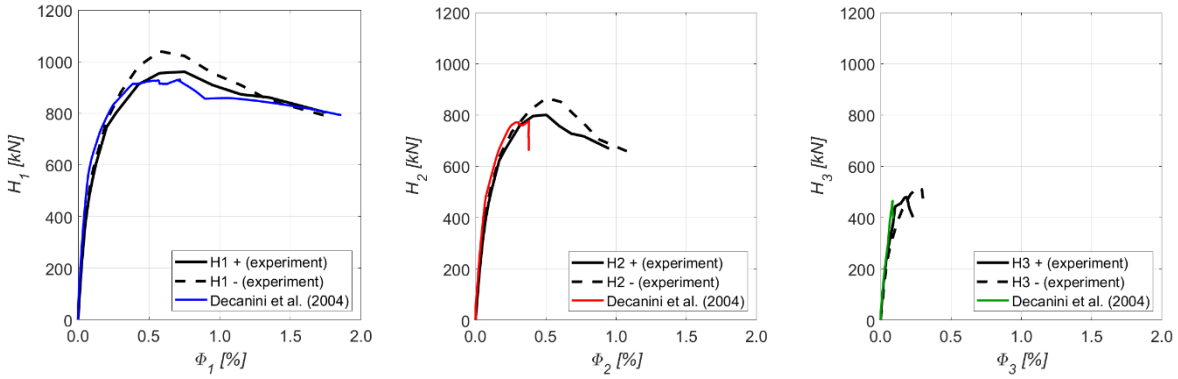

a) b) c)

Figure 12: Comparison of the numerical simulation and experimental envelope curves along the floors.

4. Conclusions

The equivalent diagonal strut models, using different constitutive laws for the struts, were analysed to determine the most suitable approach for modelling CM built from the new type of masonry and PU glue. The experimental envelope curves for both walls (average response) obtained from shear-compression tests were compared with the numerical results from the ESM models using constitutive laws (for strut) proposed by Panagiotakos and Fardis [9], Decanini et al. [10], and Liberatore et al. [11]. The results showed that the Decanini et al. model provided the best match with the experimental response, with an error in initial stiffness of 10 %, the peak load capacity underestimated by 8.8 %, and the drift at peak load capacity by only 0.1 %. Therefore, this model was used in the next phase to

DOI: https://doi.org/10.5592/CO/3CroCEE.2025.95

simulate the seismic response of the three-storey CM building, for which the actual experimental response was also known.

The response of the three-storey building model was generally well-aligned with the experiment. The pushover curve for the entire building and the ground floor was excellently captured, with the peak load capacity being underestimated for the entire building by only 3 % for pushing and 10 % for pulling. However, the seismic response of the first and second floors was somewhat less accurate. Future work will focus on refining the numerical model to better capture the damage distribution across the floors.

Acknowledgements

The research was sponsored by the Slovenian Research and Innovation Agency (programme P2-0185).

References

[1] Gams, M., Triller, P., Jäger, A. (2023): In-plane seismic behaviour of URM and confined masonry built from vertically perforated blocks and polyurethane glue, *Structures*, **58**, 105528, doi: 10.1016/j.istruc.2023.105528

[2] Gams, M., Triller, P., Tomaževič, M., Jäger, A. (2024): Test of three-storey confined masonry structure built from clay blocks and PU glue, *Journal of Building Engineering*, **91**, 109696, doi: 10.1016/j.jobe.2024.109696

[3] McKenna, F., Fenves, G. L., Scott, M. H., & Jeremic, B. (2000): Open system for earthquake engineering simulation (OpenSees). Pacific Earthquake Engineering Research Center, University of California, Berkeley, CA, USA.

[4] EN 1998-1 (2004): Eurocode 8: Design of structures for earthquake resistance – Part 1: General rules, seismic actions and rules for buildings, European Committee for Standardization.

[5] Tomaževič, M. (1999): *Earthquake-Resistant Design of Masonry Buildings*, Imperial College Press, 1st edition, London, U.K.

[6] EN 1996-1-1 (2005): Eurocode 6: Design of masonry structures – Part 1-1: General rules for reinforced and unreinforced masonry structures, European Committee for Standardization.

[7] Tarque, N., Candido, L., Camata, G., Spacone, E. (2015): Masonry infilled frame structures: State-of-the-art review of numerical modelling, *Earthquakes and Structures*, **8** (1), 225–251, doi: 10.12989/eas.2015.8.3.733

[8] Lang, A.F., Crisafulli, F.J., Torrisi, G.S. (2014): Overview and assessment of analysis techniques for confined masonry buildings, *10th National Conference in Earthquake Engineering*, Anchorage, Alaska, USA.

[9] Panagiotakos, T.B., Fardis, M.N. (1994): Proposed Nonlinear Strut Models for Infill Panels, 1st year Progress Report of HCM-PREC8 Project, University of Patras.

[10] Decanini, L., Mollaioli, F., Mura, A., Saragoni, R. (2004): Seismic performance of masonry infilled R/C frames, *13th World Conference on Earthquake Engineering 13WCEE*, Vancouver, B.C., Canada.

[11] Liberatore, L., Noto, F., Mollaioli, F., Franchin, P. (2018): In-plane response of masonry infill walls: Comprehensive experimentally-based equivalent strut model for deterministic and probabilistic analysis. *Engineering Structures*, **167**, 533-548, doi: https://doi.org/10.1016/j.engstruct.2018.04.057

[12] EN 1998-3 (2005): Eurocode 8: Design of structures for earthquake resistance – Part 3: Assessment and retrofitting of buildings, European Committee for Standardization.